Pygmy mouse songs reveal anatomical innovations underlying acoustic signal elaboration in rodents

Tobias Riede[1] and Bret Pasch[2]

[1] Department of Physiology, Midwestern University Glendale, AZ, USA
[2] Department of Biological Sciences, Northern Arizona University, Flagstaff, AZ, USA

Acknowledgement: We thank Nathaniel Mull for assistance in trapping animals in the field and Bryan Carlin for assistance with recording animals in the laboratory. The study was funded by the National Science Foundation IOS # 1755429 (BP) and # 1754332 (TR).

Author contributions: TR and BP both equally conceived the idea for the study, collected samples, performed imaging and data acquisition, analyzed the results, wrote and revised the manuscript.

Data availability: Derived 3D surfaces have been archived at Morphobank, project # 3638.

Keywords: vocal production; mammals; geometric morphometrics; contrast enhanced micro CT; ultrasonic vocalization

Summary statement

Rodents produce a variety of vocalizations to mediate social interactions, yet little is known about the mechanisms that facilitate and contribute to divergence in sound production. Northern pygmy mice produce an elaborate song through laryngeal whistling supported by a large air sac located inside the larynx, providing novel insight into the anatomical and physiological basis of signal elaboration.

Abstract

Elaborate animal communication displays are often accompanied by morphological and physiological innovations. In rodents, acoustic signals used in reproductive contexts are produced by two distinct mechanisms, but the underlying anatomy that facilitates such divergence is poorly understood. 'Audible' vocalizations with spectral properties between 500 Hz and 16 kHz are thought to be produced by flow-induced vocal fold vibrations, whereas 'ultrasonic' vocalizations with fundamental frequencies above 19 kHz are produced by an aerodynamic whistle mechanism. Baiomyine mice (genus *Baiomys* and *Scotinomys*) produce complex frequency modulated songs that span these traditional distinctions and represent important models to understand the evolution of signal elaboration. We combined acoustic analyses of spontaneously vocalizing northern pygmy mice (*B. taylori*) mice in air and light gas atmosphere with morphometric analyses of their vocal apparatus to infer the mechanism of vocal production. Increased fundamental frequencies in heliox indicated that pygmy mouse songs are produced by an aerodynamic whistle mechanism supported by the presence of a ventral pouch and alar cartilage. Comparative analyses of the larynx and ventral pouch size among four additional ultrasonic whistle-producing rodents indicate that the unusually low 'ultrasonic' frequencies (relative to body size) of pygmy mice songs are associated with an enlarged ventral pouch. Additionally, mice produced shorter syllables while maintaining intersyllable interval duration, thereby increasing syllable repetition rates. We conclude that while laryngeal anatomy sets the foundation for vocal frequency range, variation and adjustment of central vocal motor control programs fine tunes spectral and temporal characters to promote acoustic diversity within and between species.

Introduction

Advertisement signals used in reproductive contexts are among the most diverse and elaborate traits in the animal kingdom (Bradbury and Vehrencamp 2011). Understanding the mechanisms of signal production is central to understanding how signals diversify and the anatomical innovations that promote or constrain divergence. Indeed, recent work on traits used in social communication provide important insights into the processes underlying phenotypic evolution (e.g. Ord et al. 2013, Eliason et al. 2015, 2020).

Rodents produce diverse and complex vocal communication signals in a variety of social interactions (Sales, Pye 1974; Brudzynski 2018; Dent et al. 2018). Many muroid rodents are able to produce two distinct spectral ranges produced by divergent physical mechanisms (e.g., Pasch et al. 2017). Currently, sounds with spectral properties between 500 Hz and 16 kHz (hereafter 'audible sounds') are assumed to be produced by flow-induced vocal fold vibrations, whereas sounds with fundamental frequencies between 19 - 100 kHz (hereafter 'ultrasonic vocalizations, USV') are produced by a whistle mechanism (Riede 2018). This distinction is based on data from laboratory mice (*Mus musculus*) and rats (*Rattus rattus*) and does not properly reflect the large acoustic diversity among non-traditional rodent models (e.g., Miller and Engstrom 2007, 2011, Pasch et al. 2011, Pasch et al. 2017). The spectral boundary between the two production mechanisms may not be as clear or mutually exclusive. Comparative data on vocal anatomy and underlying production mechanisms is thus needed to provide insight into the evolution of acoustic communication within the largest mammalian clade.

Current understanding of rodent vocal production mechanisms indicates that spectral content is determined by laryngeal anatomy (Riede 2018). Ultrasonic whistle production appears dependent upon the presence of an intra-laryngeal air sac (ventral pouch) as well as a small cartilage (alar cartilage) that supports the ventral pouch entrance (Riede et al. 2017). The ventral pouch and the alar cartilage are located rostral from the vocal folds and have been identified in a few muroid rodents (laboratory mouse: *Mus*, laboratory rat: *Rattus*, and grasshopper mouse; *Onychomys*: Riede et al. 2017). However, both structures were absent in a heteromyid rodent (kangaroo rat; *Dipodomys*) that displays a limited vocal repertoire (Riede et al. 2017). Indeed, alterations of the ventral pouch cause changes or disappearance of ultrasonic vocal capabilities (Riede et al. 2017). Furthermore, muscle activity can regulate the position of the alar cartilage and ventral pouch size to modulate spectral features of vocalization (Riede 2013). Altogether, the

ventral pouch appears critical for ultrasonic whistle production and its size is predicted to be negatively associated with fundamental frequency of vocalizations (Riede et al. 2017).

Cricetid rodents in the subfamily Neotominae commonly produce audible (< 20 kHz) vocalizations (Miller, Engstrom 2007, 2011). Animals often assume an upright posture and open their mouths widely to generate loud vocalizations (Bailey 1931; Blair 1941; Packard 1960; Hooper and Carleton 1976) used to attract mates and repel rivals (Campbell et al. 2019; Pasch et al. 2011, 2013). Northern pygmy mice (*Baiomys taylori*) are crepuscular cricetid rodents that inhabit arid grasslands, coastal prairie mixed scrub, post oak savanna, and mesquite–cactus habitats from Texas to Mexico (Eshelman and Cameron 1987). The staccato-like song of pygmy mice is described as a ‘‘high- pitched, barely-audible squeal’’ produced with head ‘‘thrust forward and upward, stretching the throat’’ (Blair 1941, Packard 1960, Carleton 1980). Miller and Engstrom (2007) reported that songs were produced by both sexes and not as elaborate as the songs produced by sister taxa neotropical singing mice (*Scotinomys*; Pasch et al. 2011, 2013). How such frequency modulated songs are produced is unknown but promises to provide important insight into the evolution of signal elaboration in the largest radiation of mammals.

In this study, we used acoustic recordings in normal air and a light gas mixture to determine the mode of vocal production of northern pygmy mouse songs. Use of gases that are lighter or heavier than ambient air have a long tradition in the study of vocal production mechanisms (e.g., Beil 1962; Nowicki 1987; Pasch et al. 2017). Sounds produced via a whistle mechanism demonstrate a characteristic increase in fundamental frequency in helium atmosphere that is distinct from the constancy of fundamental frequencies produced via flow-induced vocal fold vibration (Spencer and Titze 2001). We then used contrast enhanced micro-CT imaging and histology to characterize the laryngeal anatomy subserving such unique sound production. Finally, we used geometric morphometrics to compare laryngeal differences within pygmy mice and among closely related species to assess the contribution of larynx and ventral pouch size and shape to acoustic diversity.

Methods

Animals

We captured northern pygmy mice near Rodeo, New Mexico, USA using Sherman live-traps baited with sterilized bird seed. Mice were transferred in standard mouse cages to animal

facilities at Northern Arizona University, Flagstaff, AZ, USA, maintained on a 14 L:10 D cycle (21 ± 2°C) and provided rodent chow, bird seed, and water *ad libitum*. A subset of animals was transferred to Midwestern University, Glendale, AZ, USA, for heliox experiments and morphological analysis. All procedures performed in studies involving animals were in accordance with the ethical standards and approval of the Institutional Animal Care and Use Committee at Midwestern University (MWU#2852) and Northern Arizona University (16-001 and 19-006) and guidelines of the American Society of Mammalogists (Sikes et al. 2016). Animals were captured with permits from the New Mexico Department of Game and Fish (3562) and the Arizona Game and Fish Department (607608).

Acoustic recording, heliox experiments, and statistical analyses

We recorded the mass and vocalizations of 10 wild-captured mice (n = 5/sex) over 10 days. Singly-housed mice in their home cage were placed in semi-anechoic coolers lined with acoustic foam. We used 1/4″ microphones (Type 40BE, G.R.A.S.) connected to preamplifiers (Type 26 CB, G.R.A.S.) to obtain recordings 33.3 cm above the center of the focal mouse cage. Microphone response was flat within ± 1.5 dB from 10 Hz to 50 kHz, and pre-amplifier response was flat within ± 0.2 dB from 2 Hz to 200 kHz. Microphones were connected to a National Instruments DAQ (USB 4431) sampling at 102.4 kHz to a desktop computer running MATLAB (Version 2018a).

We used Avisoft SASLab Pro (version 5.2.13, Avisoft Bioacoustics, Germany; 1024-point Fast Fourier Transform (FFT), 75% frame size, Hann window, frequency resolution 100 Hz, temporal resolution 93.75%, 0.625 ms) to automatically extract temporal (song duration) and spectral (maximum, and minimum fundamental frequency, and frequency bandwidth averaged across all notes in the song) parameters from each bandpass filtered (17.5-40.5 kHz) recording.

Student's t-tests were used to compare body mass, number of songs, and acoustic parameters between females and males in JMP Pro (Version 14.1.0, SAS Institute, Inc., Cary, N.C., USA). We used a Bonferroni correction to control for multiple (n= 5) comparisons (corrected $\alpha = 0.01$). We also assessed if repeatability of acoustic parameters differed between the sexes by calculating intraclass correlation coefficients (ICC; Wolak et al. 2013) using the ICC R package (version 2.3.0, Wolak 2013) in R version 3.6.1 (R Core Team 2019). Acoustic parameters were considered repeatable if the 95% confidence interval of ICC values excluded

153 zero, and similar between sexes if confidence intervals overlapped one another. Values are
154 reported as mean ± standard deviation in text.
155 Songs of six additional animals (3 songs/sex/treatment) were recorded in normal air and a
156 heliox atmosphere. Individual mice were placed in a standard mouse cage. The cage was
157 equipped with bedding, food, and water. Heliox gas (80% He, 20% O_2) was injected into the
158 cage at flow rates between 20-40 L/min through a 12 mm wide tube placed into the cage wall
159 near the floor. Predicted effects of light gas concentrations were estimated with a small whistle
160 placed at the floor of the cage and connected externally by a silastic tube. The whistle was blown
161 and recorded at regular intervals in order to monitor the heliox concentration. The ratio of the
162 frequency of the whistle in air and in heliox allowed an estimation of the expected effect for any
163 given heliox concentration.
164 Three randomly selected syllables (from the first, second, and last third of the song) from
165 each song were analyzed for minimum (F0 min), maximum (F0 max) fundamental frequency,
166 syllable duration, and relative amplitude of the first and second harmonic of the fundamental
167 frequency. While conducting the experiments, we noticed that the temporal characteristics of
168 songs changed in heliox. Therefore, we measured syllable repetition rate, syllable duration, and
169 intersyllable intervals (i.e., the duration between two adjacent syllables) for three songs in
170 normal air and in heliox. Syllable repetition rate was calculated by dividing the number of
171 syllables within a song by song duration. Syllable duration and intersyllable intervals were
172 averaged over all syllables of a song. Acoustic differences between normal air and heliox songs
173 were assessed with paired t-tests.
174
175 *Histology, CT scanning and 3D rendition of the larynx*
176 Ten mice (5/sex) were euthanized with isoflurane and then transcardially perfused first
177 with saline solution followed by 10% buffered formalin. Larynges were dissected and placed in
178 10% buffered formalin phosphate (SF100-4; Fisher Scientific) for two days.
179 Four specimens (2/sex) were used to prepare histological sections. Mid-membraneous
180 coronal sections (5 mm thick) were stained with haematoxylin-eosin for a general overview. We
181 also attempted to use Masson's Trichrome (TRI) for collagen fiber stain and Elastica-Van
182 Gieson (EVG) for elastic fiber stain. However, pygmy mouse vocal folds are small (see below),
183 and we were unsuccessful in collecting a sufficient sample size of mid-membraneous sections for

184 different stains in each individual. Sections were scanned with an Aperio CS 2 slide scanner and
185 processed with Imagescope software (v. 8.2.5.1263; Aperio Tech.).
186 Two specimens (1/sex) were whole-body scanned at 50 µm resolution. Larynges from
187 these two individuals and four additional mice (3/sex) were also x-rayed at 5 µm resolution.
188 First, tissues were transferred from the formalin solution to 99% ethanol. Tissues were then
189 stained in 1% phosphotungstic acid (PTA) (Sigma Aldrich, 79690) in 70% ethanol. After 5 days,
190 the staining solution was renewed and the tissue was stained for another 5 days. After staining,
191 specimens were placed in a custom-made acrylic tube and scanned in air. CT scanning was done
192 using a Skyscan 1172 (Bruker). Reconstructed image stacks were then imported into AVIZO
193 software (version Lite 9.0.1). Laryngeal cartilages and the border between the airway and soft
194 tissues of the larynx in the CT scans were traced manually. This approach provided outlines of
195 the cartilaginous framework and the airway. Derived 3D surfaces of all six specimen have been
196 archived at Morphobank (O'Leary, Kaufman 2012), project # 3638.
197
198 *Geometric morphometric analysis of laryngeal shape*
199 We investigated whether the laryngeal size or shape of *Baiomys* mice were sexually
200 dimorphic using a geometric morphometric (GM) approach. 3D surfaces of three male and three
201 female laryngeal cartilages were used to quantify shape using curve and surface landmarks.
202 Landmarks were placed on surface renderings using the 'geomorph' package, Version 3.0.5.
203 (Adams et al. 2017) for the R software package (R Development Core Team 2008). Fixed
204 landmarks were placed along the cartilage border and supplemental by 100 surface
205 semilandmarks, which were placed with help of an interactive function to build a template of 3D
206 surface semilandmarks. In order to compare cartilage shape, a generalized Procrustes analysis
207 was used to remove variation related to position, size, and orientation. Next, we employed a
208 series of principal components analyses (PCA), to summarize the main patterns of shape
209 variance in the data. The procedure used here has been previously established (Borgard et al.
210 2019).
211 Centroid size was used to estimate overall size for each cartilage. Centroid size is the
212 square root of the sum of squared distances of each landmark from the center of the cartilage.
213 The location is obtained by averaging the *x, y* and *z* coordinates of all landmarks (Zelditch et al.,
214 2004).

For comparative analyses, we used data from laboratory mice (*Mus musculus*), laboratory rats (*Rattus rattus*), and grasshopper mice (*Onychomys* spp.) published previously by Borgard et al. 2019. To assess whether laryngeal cartilage shape exhibited sex differences in pygmy mice, we performed a multivariate analysis of variance (MANOVA) on the PC 1 and PC 2 scores for each cartilage.

Results

Baseline acoustic recording

Long-distance songs consisted of repeated frequency modulated syllables (Figure 1A). All song parameters were repeatable within individuals and between the sexes (Table 1). We found no sex differences in mass (females: 9.95 ± 1.1 g; males: 9.22 ± 0.8 g; $t_8 = -1.23$, $P = 0.25$) nor number of songs produced (females: 53 ± 52.3 songs; males: 162.8 ± 134.6 songs; $t_8 = 1.69$, $P = 0.13$; Table 1) despite males showing higher variation in song rate (range: 84-401 songs) than females (range: 5-132 songs). Males produced longer songs with slightly lower minimum F_0 and larger frequency bandwidths compared to females (Table 1). (female song duration ICC: 0.19, 95% CI, 0.06-0.68; male song duration ICC: 0.13, 95% CI, 0.05-0.56).

Heliox experiments

Both maximum and minimum F_0 increased in heliox (paired *t*-test, Max F_0: $t = -10.0$, $p < 0.001$; Min F_0: $t = -14.1$, $p < 0.001$) compared to normal air (Figure 1B - D). However, the amplitude of higher harmonics ($2F_0$) in normal air and in heliox relative to F_0 at the center of syllables did not differ (paired *t*-test, $t = -1.3$, $p = 0.261$; Figure 1E).

While song duration and intersyllable intervals did not differ between normal air and heliox (paired *t*-test, song duration: $t = 0.70$, $p = 0.513$; intersyllable interval: $t = 0.61$, $p = 0.566$; Figure 2 A and B), other temporal features of the song changed in heliox. Syllable duration decreased significantly (paired *t*-test, $t = 5.5$, $p < 0.01$) and, since intersyllable intervals were unaltered, syllable repetition rate increased (paired *t*-test, $t = -4.6$, $p < 0.01$) (Figure 2 C and D). Figures 2 E and F show individual syllable durations over the course of three songs in normal air and in heliox, for a male and a female mouse, respectively. Syllable duration decreased by 15 ± 6.7% (mean ± stdev) and syllable repetition rate increased 10.5 ± 4.4%, yet the number of

246 syllables per song did not change significantly (# syllables$_{AIR}$ = 28.9 ± 4.6; (# syllables $_{HELIOX}$ =
247 29.5 ± 6.9; t = 0.88, p = 0.422) (Figure 2F).
248
249 *Pygmy mouse vocal morphology*
250 The membraneous portion of a vocal fold (captured by six subsequent sections in Figure
251 3A – F) refers to the soft tissue that starts at the vocal process of the arytenoid cartilage and ends
252 where the vocal fold attaches to the interior of the thyroid cartilage. The ventral section of the
253 membraneous portion of the vocal fold is re-enforced with cartilaginous tissue and is continuous
254 with the alar cartilage and epiglottis. Consequently, the cartilaginous free, membraneous portion
255 of the vocal fold is very short (< 150 ± 24 μm; n = 4). The membraneous portion of the vocal
256 fold is composed of thyroarytenoid muscle, lamina propria, and epithelium. The lamina propria
257 of the membraneous portion is comprised of a thick layer (up to 110 ± 1.5 μm SD) of collagen
258 and elastic fibers (Figure 3G).
259 The ventral pouch of *Baiomys* is large with a medially-positioned portion rostral from the
260 vocal folds (Figure 4A). Additionally, pockets connected to the medial portion extend laterally
261 from each vocal fold, causing a unique morphology of the ventral portion of the vocal fold
262 unprecedented in the mammalian larynx (e.g., Negus 1949; Schneider 1964). The vocal fold is
263 very thin and membranous (Figures 3 C-F). The alar cartilage forms the edge of the entrance into
264 the ventral pouch. Figures 3 H and I illustrate the cartilage. Histological sections demonstrate
265 that the cartilage is associated with the epiglottis (Figure 3 I).
266 The thyroid cartilage consists of a left and right lamina each with a rostral and caudal
267 horn (Figure 5A-D). The rostral horn is narrow and pointed. The rostro-ventral margin of the
268 thyroid bends dorsally, toward the laryngeal lumen forming a *Bulla thyroidea* (Figure 5D). The
269 ventral pouch is embedded in this bulla. A small cartilaginous protuberance is present on the
270 medial surface of the thyroid cartilage in a caudal midsagittal position (Figure 5B). The structure
271 consists of highly mineralized cartilage that protrudes into the laryngeal lumen. Vocal folds
272 attach to the thyroid cartilage via this protuberance.
273 The cricoid cartilage (Figure 5 E-H) forms a complete ring with a broad plate dorsally
274 and a narrow band laterally and ventrally. The arytenoid cartilages form triangular shaped
275 structures with a vocal process, a short muscular process and a long and narrow dorsal process
276 (aka *apex*) (Figure 5 I-L). The epiglottis (Figure 5 M-P) forms a small sheet bending towards the

277 airway. Most notable is the structure at the caudal end of the epiglottis, which is described as alar
278 cartilage in other species. In *Mus*, *Rattus* and *Onychomys*, the alar cartilage was a separate
279 structure without connection to another laryngeal cartilage (Riede et al. 2017). In *Baiomys*, the
280 alar cartilage supports the entrance into the ventral pouch and is moved by fibers from the
281 thyroarytenoid muscle. Unlike in *Mus*, *Rattus* or *Onychomys*, the alar cartilage is tightly
282 connected with the epiglottis in *Baiomys*.
283 The length of oral and pharyngeal cavity (vocal tract length measured between vocal fold
284 and tip of incisivi) measured 16 and 17 mm in a female and male specimen, respectively, for
285 which the whole body was scanned before the larynx was excised for high-resolution scanning.
286
287 *Analysis of larynx size and shape*
288 Laryngeal size represents an important source of spectral differences in animal
289 vocalizations. We therefore investigated the size and shape of laryngeal cartilages as well as the
290 ventral pouch. First, we tested for morphological differences between sexes in *Baiomys*, and then
291 compared larynx size of *Baiomys* to *Mus*, *Rattus* and *Onychomys* in order to explain the
292 fundamental frequency of *Baiomys* songs.
293 Neither the size of the four laryngeal cartilages nor any of the ventral pouch dimensions
294 demonstrated sexual dimorphism in *Baiomys* (Table 2). Cartilage shape was also not different
295 between the sexes. None of the four cartilages exhibited separation of their shape along the first
296 or second principal component (PC 1 and PC 2) (thyroid cartilage: $F_{1, 3} = 0.88$, p=0.21; Wilk's
297 $\Lambda = 0.82$; cricoid cartilage: $F_{1, 3} = 0.89$, p=0.21; Wilk's $\Lambda = 0.82$; arytenoid cartilage: $F_{1, 3} =$
298 0.85, p=26; Wilk's $\Lambda = 0.78$; epiglottis: $F_{1, 3} = 0.64$, p=0.84; Wilk's $\Lambda = 0.51$) (Figure 6 A-D).
299 Compared to three other species, *Baiomys* possesses a very large and unusually shaped
300 ventral pouch (Figure 7 A-D). Overall larynx size remains linked to body size (Figure 7 E-H).
301 All four cartilages scaled with negative allometry against body mass. Interestingly, the size of the
302 ventral pouch, a structure which is located inside the larynx, is not linked to larynx size or body
303 size (Figure 7 I – J). However, ventral pouch dimension, in particular its latero-lateral width,
304 appears to be associated with the fundamental frequency among the four species (Figure 7 K).
305
306 **Discussion**

Our findings indicate that the elaborate singing behavior of baiomyine mice arises from a unique laryngeal morphology that facilitates aerodynamic whistle production. In particular, a large air sac termed the ventral pouch and a robust alar cartilage is associated with the production of fundamental frequencies through an aerodynamic whistle. In rodents, presence of a ventral pouch and alar cartilage are associated with ultrasonic whistle production, and damage to the alar cartilage and ventral pouch compromises whistle fidelity (Riede et al. 2017). Our current findings further support the association between the presence of a ventral pouch and alar cartilage with the ability to produce ultrasonic vocalizations by an aerodynamic whistle mechanism. More specifically, comparative analyses indicate that ventral pouch size is associated with fundamental frequency, allowing relatively small species to produce low frequency songs independent of body size. Our findings provide important insight into the anatomical innovations that facilitate signal elaboration.

The relatively low fundamental frequencies of pygmy mouse songs are remarkable because they are among the smallest rodents (8-12 g; Wilson and Reeder 2005). The songs extend to the lowest aerodynamic whistle frequency recorded among four species for which anatomical information and light gas experiments have informed our understanding of the vocal production mechanisms. From one perspective, pygmy mouse ultrasonic whistles overlap the audible calls of grasshopper mice, a genus that is larger in mass (32 - 38g) and produces long-distance vocalizations using vocal fold vibrations (Pasch and Riede 2017). Conversely, pygmy mouse frequencies also overlap with the lowest ultrasonic frequencies reported for laboratory rats (19 kHz; Brudzynski et al. 1993; Wright et al. 2010), which are 10-20 times larger than pygmy mice (250 to 500 g; Wilson and Reeder 2005). In addition, pygmy mouse song frequencies are much lower than those of laboratory mouse (*Mus musculus*) songs (Holy and Guo 2005), a species that is slightly larger (25 to 50 g; Wilson and Reeder 2005), but whose ventral pouch is much smaller than *Baiomys* (Riede et al. 2017; herein). Thus, while the overall size of the vocal apparatus appears to scale linearly with body size (Figure 7 E-H), dimensions of the ventral pouch uncouples the relationship between body size and size-dependent acoustic features (Figure I-K).

The fundamental frequency of USVs depends on glottal airflow velocity, the distance between the glottal and alar edge, and ventral pouch volume (Riede et al. 2017). Our data suggest that laryngeal cartilage size scaled allometrically with body size but was not associated

with vocal frequencies. In contrast, ventral pouch size was inversely related to maximum and minimum fundamental frequency across species and likely explains the low frequency range of *Baiomys* songs. While the ventral pouch did not explain sexual dimorphism of acoustic features in the songs of pygmy mice, the slight difference (2 kHz) in spectral content between the sexes may be too minimal to detect with our methodology. Alternatively, sex differences in muscle tension may contribute to laryngeal shape and size differences that mediate vocal output (Riede 2013).

Air sacs, ventricles, bullae, and ventral pouches

Side branches or cavities branching off of the main upper airway above and below the laryngeal valve are common in mammals and birds (e.g., King, McLelland 1984; Riede et al. 2008). Such rigid or inflatable cavities serve to amplify sound levels, modify existing resonance properties, or introduce an additional resonance frequency (Riede et al. 2008; deBoer 2009). In rodents, the air sac or ventral pouch is different than airsacs in nonhuman primates, cervids, and birds. Whereas non-rodent airsacs can branch off of the airway above or below the glottis, the rodent ventral pouch is always positioned rostral to the glottis, embedded inside the thyroid cartilage lumen, and supported by cartilaginous structures. The alar cartilage or modifications of the epiglottis reinforce the entrance and lateral wall of the ventral pouch. Riede et al. (2017) suggested that the alar edge of the reinforced entrance acts like the blade or labium of the air hole of a recorder. The glottal airflow is guided over the ventral pouch entrance and hits the alar edge which opposes the glottis, generating pressure fluctuations that presumably excite resonances inside the ventral pouch. In addition, the alar cartilage is associated with a small body of muscle fibers branching off from the thyroarytenoid muscle, and activity of this muscle is precisely associated with fundamental frequency features of vocalizations (Riede 2013). Together, our anatomical findings suggest that the dimensions of rodent ventral pouch, unlike other airsacs, are precisely controlled.

Vocal-respiratory coordination

Most heliox studies in bioacoustics focus on spectral analysis because resultant patterns are indicative of underlying production mechanisms. We hypothesize that heliox experiments can also inform our understanding of vocal-respiratory coordination. In particular, we found that

pygmy mouse syllables were shorter in duration in heliox than in air. Our findings are in accordance with heliox-induced shortening of vocalizations in grasshopper mice (*Onychomys*; Pasch et al. 2017) and common marmosets (*Callithrix jacchus;* Zhang, Ghazanfar 2018) that both produce vocalizations by airflow-induced vocal fold vibration. The magnitude of the effect was similar among species (*Baiomys*, 15%; *Onychomys*, 19%; *Callithrix,* 11%). We speculate that the lower density of inhaled heliox affects laryngeal aerodynamics by an eased gas flow through the constricted glottal valve during vocal production (Sundberg 1981). Consequently, a slightly reduced air volume is available during expiration to decrease syllable duration. Confirmation of this hypothesis will require further experimentation with varying concentrations of light gas and/or use of heavy gas.

Our findings provide further insight into vocal-respiratory coordination when contextualized in relation to recent work in another baiomyine rodent (Alston's singing mouse; *Scotinomys teguina*) that produces a similar repetitive song (e.g., Campbell et al. 2010; Pasch et al. 2011). Okobi et al. (2019) found that cooling of the orofacial motor cortex decreased the rate of change of syllable duration without affecting the duration of individual syllables. While not explicitly stated, cooling appears to do so by increasing the duration of the inhalation phase (i.e. intersyllable intervals), which directly contrasts our heliox findings that show an impact on the expiratory phase (syllable duration) without changing intersyllable intervals. Together, available data suggest that songs emerge from a motor pattern coded by a central pattern generator in the brainstem (Tschida et al. 2019) whose timing is modulated by cortical control of breathing (specifically the inhalation phase) (Okobi et al. 2019). Differences in the acoustic output, however, can also simply be the result of mechanical constraints of the peripheral organ, for example laryngeal aerodynamics that are sensitive to airflow (this study). Integration of laryngeal and breathing movements coupled with a detailed understanding of vocal organ morphology and laryngeal aerodynamics provides a fuller understanding of the nature of rodent acoustic signals and their evolution.

Conclusions

Ultimately, understanding how acoustic characters evolve requires knowledge of how signals are produced. Our findings indicate that diversity in the size of a unique laryngeal structure termed the vocal pouch is associated with extreme divergence in fundamental

frequencies of ultrasonic whistles. Thus, the traditional approach of categorizing vocal signals by spectral range into "audible" (up to 16 kHz) and "ultrasonic" (above 19 kHz) vocalizations requires revision. Indeed, the challenge of differentiating 'audible' and 'ultrasonic' vocalizations in rodents has been noted (e.g., Grimsley et al. 2016; Kalcounis-Rueppell 2010, 2018; Miller and Engstrom 2007, 2011, 2012). A production-based definition that distinguishes between flow-induced vocal fold vibration and aerodynamic whistles provides a more robust framework to explore diversification of rodent voices. Heliox experiments confirmed that the ultrasonic songs in pygmy mice are aerodynamic whistles and can reach low into the 'sonic' frequency range. Other species may have adaptations that may extend the spectral range of whistles to low frequencies (this study) or the range of flow-induced vocal fold vibrations into exceptionally high spectral regions (e.g., Titze et al. 2018). The study also informs our understanding of the vocal production mechanism which requires precise coordination between three systems (larynx, breathing, and vocal tract). Aerodynamics at the vocal folds (vibrating or not) are determined not only by the coordination of the three systems but also by the laryngeal morphology and biomechanical properties.

Altogether, the current study demonstrates that rodents are a promising system for understanding how mechanisms of complex behaviors like vocal production may promote or constrain divergence.

References

Adams, D. C., Collyer, M. L., Kaliontzopoulou, A., and Sherratt, E. (2017). Geomorph: Software for geometric morphometric analyses. R package version 3.0.5. (https://cran.r-project.org/package=geomorph.)

Bailey, V. (1931). Mammals of New Mexico. *N. Amer. Fauna*. 53, 422 pp.

Beil, R.G. (1962). Frequency analysis of vowels produced in a helium-rich atmosphere. J Acoust Soc Am 34, 347-349.

Blair, F. (1941). Observations on the life history of *Baiomys taylori subater*. *J. Mammal.,* 22, 378-383.

Borgard, H., Baab, K., Pasch, B., and Riede, T. (2019). The shape of sound: A geometric morphometrics approach to larynx morphology. *J Mammal. Evol*., https://doi.org/10.1007/s10914-019-09466-9

Bradbury, J.W., and Vehrencamp, S.L. (2011). Principles of animal communication (2nd edition). Sunderland, MA: Sinauer Associates.

Brudzynski, S.M., Bihari. F., Ociepa, F., and Fu, X. 1993. Analysis of 22 kHz ultrasonic vocalization in laboratory rats: long and short calls. *Physiol Behav*., *54*, 215–221.

Brudzynski, S.M. (2018). Handbook of Ultrasonic Vocalization. A Window into the Emotional Brain. Volume 25.

Campbell, P., Pasch, B., Pino, J.L., Crino, O.L., Phillips, M., and Phelps, S. (2010), Geographic variation in the songs of Neotropical singing mice: testing the relative importance of drift and local adaptation. *Evolution, 64*: 1955–1972.

Campbell, P., Arévalo, L., Martin, H., Chen, C., Sun, S., Rowe, A.H., Webster, M.S., Searle, J.B., and Pasch, B. (2019.) Vocal divergence is concordant with genomic evidence for strong reproductive isolation in grasshopper mice (*Onychomys*). *Ecol. Evol*., *9*, 12886-12896.

Carleton, M.D. (1980). Phylogenetic relationships in neotomine–peromyscine rodents (Muroidea) and a reappraisal of the dichotomy within New World Cricetinae. *Miscell. Publ., Museum of Zool., Univ. of Michigan*, *157*, 1-146.

Dent, M.L., Fay, R.R., and Popper, A.N. (2018). Rodent Bioacoustics. Springer Handbook of Auditory Research book series (SHAR, volume 67).

Eliason, C.M., Maia, R., Parra, J.L., and Shawkey, M.D. (2020). Signal evolution and morphological complexity in hummingbirds. *Evol., 74*, 447-458.

Eliason, C.M., Maia, R., and Shawkey, M.D. (2015). Modular color evolution facilitated by a complex nanostructure in birds. *Evol., 69*, 357-367.

Eshelman, B. D., and Cameron, G. N. (1987). *Baiomys taylori*. Mammal. Species, *285*, 1-7.

Grimsley, J., Sheth, S., Vallabh, N., Grimsley, C.A., Bhattal, J., and Latsko, M. (2016). Contextual modulation of vocal behavior in mouse: newly identified 12 kHz "mid-frequency" vocalization emitted during restraint. *Front. Behav. Neurosci., 10*, 38.

Hooper, E.T., and Carleton, M. D. (1976). Reproduction, growth and development in two contiguously allopatric rodent species, genus *Scotinomys*. *Misc. Publ. Mus. Zool., Univ. Mich*., *151*, 1–52.

Holy T.E., and Guo Z (2005). Ultrasonic songs of male mice. *PLoS Bio,* 3, e386.

Kalcounis-Rueppell, M.C., Petric, R., Briggs, J.R., Carney, C., Marshall, M.M., Willse, J.T., Rueppell, O., Ribble, D.O., and Crossland, J.P. (2010). Differences in ultrasonic vocalizations between wild and laboratory California mice (*Peromyscus californicus*). *PloS one, 5*, e9705.

Kalcounis-Rueppell, M.C., Petric, R., and Marler, C. (2018). The bold, silent type: predictors of ultrasonic vocalizations in the genus *Peromyscus*. *Front. Ecol. Evol., 6*, 198.

Light, J., Ostroff, M., and Hafner, D. (2016). Phylogeographic assessment of the northern pygmy mouse, *Baiomys taylori*. *J. Mammal., 97*, 1081-1094.

Miller, J.R., and Engstrom, M.D. (2007). Vocal stereotypy and singing behavior in Baiomyine mice. *J. Mammal., 88*, 1447-1465.

Miller, J.R., and Engstrom, M.D. (2010). Stereotypic vocalizations in harvest mice (*Reithrodontomys*): Harmonic structure contains prominent and distinctive audible, ultrasonic, and non-linear elements. *J. Acoust. Soc. Am., 128*, 1501-1512.

Miller, J.R., and Engstrom, M.D. (2012). Vocal stereotypy in the rodent genera *Peromyscus* and *Onychomys* (Neotominae): taxonomic signature and call design. *Bioacoustics, 21*, 193-213.

Negus, V.E. (1949). The comparative anatomy and physiology of the larynx. New York: Grune&Stratton, Inc.

Nowicki, S. (1987). Vocal tract resonances in oscine bird sound production: Evidence from birdsongs in a helium atmosphere. *Nature*, 325, 53–55.

O'Leary, M.A. and Kaufman, S.G. *(*2012). MorphoBank 3.0: Web application for morphological phylogenetics and taxonomy. http://www.morphobank.org

Okobi, Jr., D.E., Banerjee, A., Matheson, A.M.M., Phelps, S.M., and Long, M.A. 2019. Motor cortical control of vocal interaction in neotropical singing mice. *Science, 683,* 983-988.

Ord, T.J., Collar, D.C., and Sanger, T.J. (2013). The biomechanical basis of evolutionary change in a territorial display. *Func. Ecol., 27*, 1186-1200.

Pasch, B., George, A.S., Hamlin, H.J., Guillette, L.J., and Phelps, S.M. (2011). Androgens modulate song effort and aggression in Neotropical singing mice. *Horm. Behav., 59*, 90-97.

Pasch, B., Bolker, B.M., and Phelps, S.M. (2013). Interspecific dominance via vocal interactions mediates altitudinal zonation in neotropical singing mice. *Am. Nat., 182*, E161-E173.

Pasch, B., Tokuda, I.T., and Riede, T. (2017). Grasshopper mice employ distinct vocal production mechanisms in different social contexts. *Proc. Roy. Soc. Lond. B, 284*, 20171158.

Packard, R.L. (1960). Speciation and evolution of the pygmy mice, genus *Baiomys*. *Univ of Kansas Publ. Museum of Nat. Hist.* 9, 579-670.

Riede, T. (2013). Stereotypic laryngeal and respiratory motor patterns generate different call types in rat ultrasound vocalization. *J Exp Zool A, 319*, 213–224.

Riede, T., Borgard, H.L., and Pasch, P. (2017). Laryngeal airway reconstruction indicates that rodent ultrasonic vocalizations are produced by an edge-tone mechanism. *Royal Soc. Open Sci., 4*, 170976.

Riede, T. (2018). Peripheral vocal motor dynamics and combinatory call complexity of ultrasonic vocal production in rats. In Handbook of Ultrasonic Vocalization, edited by Stefan M. Brudzynski; Elsevier series 'Handbook of Behavioral Neuroscience', Vol 25, pp. 45-60.

Sales, G.D., and Pye, D. (1974). Ultrasonic communication by animals. Chapman & Hall, London, United Kingdom.

Schneider, R. (1964). Der Larynx der Säugetiere. *Handbuch der Zoologie*, *5*(7), 1–128.Titze, I.,Riede, T., Mau, T. (2016). Predicting achievable fundamental frequency ranges in vocalization across species. *PLoS Comput Biol*, 2, e1004907.

Spencer, M.L., and Titze, I.R. (2001). An investigation of a modal-falsetto register transition hypothesis using helox gas. *J. Voice*, 15, 15–24.

Sundberg J. (1981). Formants and fundamental frequency control in singing. An experimental study of coupling between vocal tract and vocal source. *Acoustica*, 49,48-54.

Tschida, K., Michael, V., Takato, J., Han, B.X., Zhao, S., Sakurai, K., Mooney, R., and Wang, F. (2019). A specialized neural circuit gates social vocalizations in the mouse. *Neuron*, 103, 1–14.

Wilson, D. E., and Reeder, D. M. (eds.). (2005). Mammal Species of the World: A Taxonomic and Geographic Reference. 3rd edition. Johns Hopkins University Press, Baltimore, Maryland.

Wolak, M.E., Fairbairn, D.J., and Paulsen, Y.R. (2012). Guidelines for estimating repeatability. *Methods Ecol. Evol*., *3*, 129-137.

Wright, J.M., Gourdon. J.C., and Clarke, P.B.S. (2010). Identification of multiple call categories within the rich repertoire of adult rat 50-kHz ultrasonic vocalizations: effects of amphetamine and social context. *Psychopharmacology, 211*, 1–13.

Zelditch, M.L., Lundrigan, B.L., and Garland, T. Jr. (2004). Developmental regulation of skull morphology. I. Ontogenetic dynamics of variance. *Evol. Dev., 6*, 194-206.

Zhang, Y.S., and Ghazanfar, A.A. (2018). Vocal development through morphological computation. *PLoS Biol, 16*, e2003933.

528 **Table 1:** Average (± standard deviation) parameters and repeatability estimates for female and
529 male northern pygmy mice (*Baiomys taylori*) vocalizations (n = 5/sex). Bolded *P* values reflect
530 significance following a Bonferroni correction for multiple comparisons.

Parameter	**female**	**male**	**df**	**t**	***P***	**Repeatability (95% C.I.)** **All, females, males**
Body mass (g)	9.95 ± 1.1	9.22 ± 0.8	8	-1.23	0.25	-
Number of songs	53 ± 52.3	162.8 ± 134.6	8	1.69	0.13	-
Duration (s)	3.4 ± 0.4	4.9 ± 0.5	8	4.99	**0.001**	0.37 (0.21-0.66) 0.19 (0.06-0.68) 0.13 (0.05-0.56)
Maximum fundamental frequency (kHz)	33.8 ± 2.2	33.1 ± 1.3	8	-0.68	0.52	0.63 (0.44-0.85) 0.77 (0.54-0.97) 0.61 (0.36-0.93)
Minimum fundamental frequency (kHz)	23.5 ± 1.9	21.0 ± 1.0	8	-2.51	0.046	0.63 (0.44-0.85) 0.66 (0.4-0.94) 0.44 (0.22-0.87)
Fundamental frequency bandwidth (kHz)	10.4 ± 0.5	12.1 ± 1.3	8	2.58	0.048	0.65 (0.47-0.86) 0.1 (0.03-0.53) 0.59 (0.33-0.92)

531
532

Table 2: Average (± standard deviation) parameters for female and male northern pygmy mice (*Baiomys taylori*) laryngeal cartilage size (n = 3/sex). CS, centroid size; LL, latero-lateral; VD, ventro-dorsal; CC, cranio-caudal; A1, distance between glottis and alar edge of ventral pouch entrance.

Parameter	**female**	**male**	**df**	***F***	***P***
Log_{10}(CS Thyroid cartilage)	4.03 ± 0.01	4.03 ± 0.01	1, 6	0.17	0.70
Log_{10}(CS Cricoid cartilage)	3.85 ± 0.01	3.85 ± 0.01	1, 6	0.01	0.99
Log_{10}(CS Arytenoid cartilage)	3.43 ± 0.03	3.42 ± 0.01	1, 6	0.09	0.93
Log_{10}(CS Epiglottis)	3.49 ± 0.03	3.43 ± 0.04	1, 6	3.7	0.13
Ventral Pouch LL (mm)	963 ± 116	935 ± 38	1, 6	0.15	0.71
Ventral Pouch VD (mm)	355 ± 71	386 ± 28	1, 6	0.50	0.52
Ventral Pouch CC (mm)	876 ± 38	856 ± 95	1, 6	0.11	0.75
Ventral Pouch A1 (mm)	568 ± 164	550 ± 173	1, 6	0.18	0.90

539 **Table 3**: Pearson correlation coefficients for three spectral parameters and body mass, laryngeal
540 size and ventral pouch size. The correlation between the latero-lateral (LL) dimension of the
541 ventral pouch and minimal fundamental frequency reached the greatest association.

	F0 Min	**F0 Max**	**F0 Mean**
Log10(body mass)	R = -0.33, P = 0.67	R = 0.40, P = 0.60	R = 0.28, P = 0.72
Log_{10}(CS Thyroid)	R = -0.29, P = 0.71	R = 0.41, P = 0.59	R = 0.29, P = 0.71
Log_{10}(CS Cricoid)	R = -0.29, P = 0.71	R = 0.44, P = 0.56	R = 0.32, P = 0.68
Log_{10}(CS Arytenoid)	R = -0.24, P = 0.75	R = 0.49, P = 0.51	R = 0.37, P = 0.63
Log_{10}(CS Epiglottis)	R = 0.29, P = 0.71	R = 0.73, P = 0.27	R = 0.67, P = 0.33
VP-LL	**R = -0.87, P = 0.13**	R = -0.52, P = 0.48	R = -0.61, P = 0.39
VP-DV	R = -0.42, P = 0.58	R = 0.20, P = 0.79	R = 0.09, P = 0.91
VP-CC	R = -0.54, P = 0.46	R = 0.15, P = 0.85	R = 0.02, P = 0.98
VP-A1	R = -0.07, P = 0.97	R = 0.64, P = 0.36	R = 0.54, P = 0.46

542
543

Figure Captions

Figure 1: **A**: Representative spectrograms of a female and a male northern pygmy mouse (*Baiomys taylori*) long-distance vocalization (song). The song consists of multiple frequency modulated syllables. **B**: Representative songs of a pygmy mouse in air and in a helium-oxygen mixture (heliox). Note the increase in fundamental frequency in heliox. Y-axis is different than in A. **C**: Minimum fundamental frequency ($F0_{MIN}$) for 6 animals in air in heliox; **D**: maximum fundamental frequency ($F0_{MAX}$) for 6 animals in air in heliox; **E**: relative amplitude (ratio of 2F0/F0) for 3 songs in n = 3 females (F1 – F3) and 3 males (M1 – M3).

Figure 2: Temporal features of song in air and heliox. **A**: Song duration, B: intercall intervals, **C**: syllable duration and **D**: syllable repetition rate over the entire song. Shown are means and standard deviations. Syllable duration was consistently shorter in heliox. **E** and **F** shows syllable durations across three songs in air and three in heliox for a female (**E**) and a male (**F**).

Figure 3: Coronal serial sections through the larynx of a male pygmy mouse (**A** – **F**, dorsal to ventral). The sections are 50 microns apart. In **B**, there is still part of the arytenoid cartilage present in the vocal fold. The membraneous portion of the vocal fold (i.e., no cartilage present) is shown in **D** and **E**. Then, in **F**, cartilage is present which is part of the alar cartilage. The lateral pocket of the ventral pouch is visible in sections **C** through **F**. The inset in **B** is magnified in **G**. The inset in **F** is magnified in **H**. **I**: The image is taken from a section subsequent to **F.** It shows that the cartilage in the vocal fold is part of the alar cartilage. Furthermore it shows that the alar cartilage is connected to the epiglottis.
Scale bar in **F** applies to **A** –**F**. Scale bar in **H** applies to **H** and **I**. E, epiglottis; T, thyroid cartilage; VF, vocal fold; TA, thyroarytenoid muscle; LP, lamina propria of the vocal fold.

Figure 4: **A**: Lateral view of a mid-sagittal section through the 3D reconstruction of laryngeal cartilages and laryngeal airway of a male pygmy mouse. The dashed line indicates the position of

575 the cranial edge of the vocal fold. **B**: CT image of midsagittal view of a female pymy mouse
576 larynx. **C – E**: Three-dimensional surface rendition of the airway in four different views. A,
577 arytenoid cartilage; E, epiglottis; T, thyroid cartilage; VP, ventral pouch; C, cricoid cartilage.
578
579
580 **Figure 5**: Three dimensional surface renditions of laryngeal cartilages of a male northern pygmy
581 mouse. A-D: thyroid cartilage. E-H: cricoid cartilage I-L: arytenoid cartilage. M-P: Epiglottis
582
583
584 **Figure 6**: **A-D**: Principal component analysis of the Procrustes shape coordinates from curve and
585 surface semilandmarks. Each point represents the cartilage shape of one individual (closed
586 circles males; open circles females). **E-H**: Relationships between cartilage size (measures as
587 'centroid size) and body mass.
588
589
590 **Figure 7:** *Baiomys* possesses large ventral pouch. **A – D**: Cranio-caudal views of the ventral
591 pouch of four rodent species which produce ultrasonic whistles. Solid black bars are 1 mm. **E -**
592 **H**: Relationships between body mass and centroid size of thyroid, cricoid, arytendoid cartilage
593 and epiglottis.
594 Relationships between minimum fundamental frequency of ultrasonic vocalizations and body
595 mass (**I**), between body mass and ventral pouch size (latero-lateral dimension) (**J**), and between
596 ventral pouch size and minimum fundamental frequency (**K**).
597
598

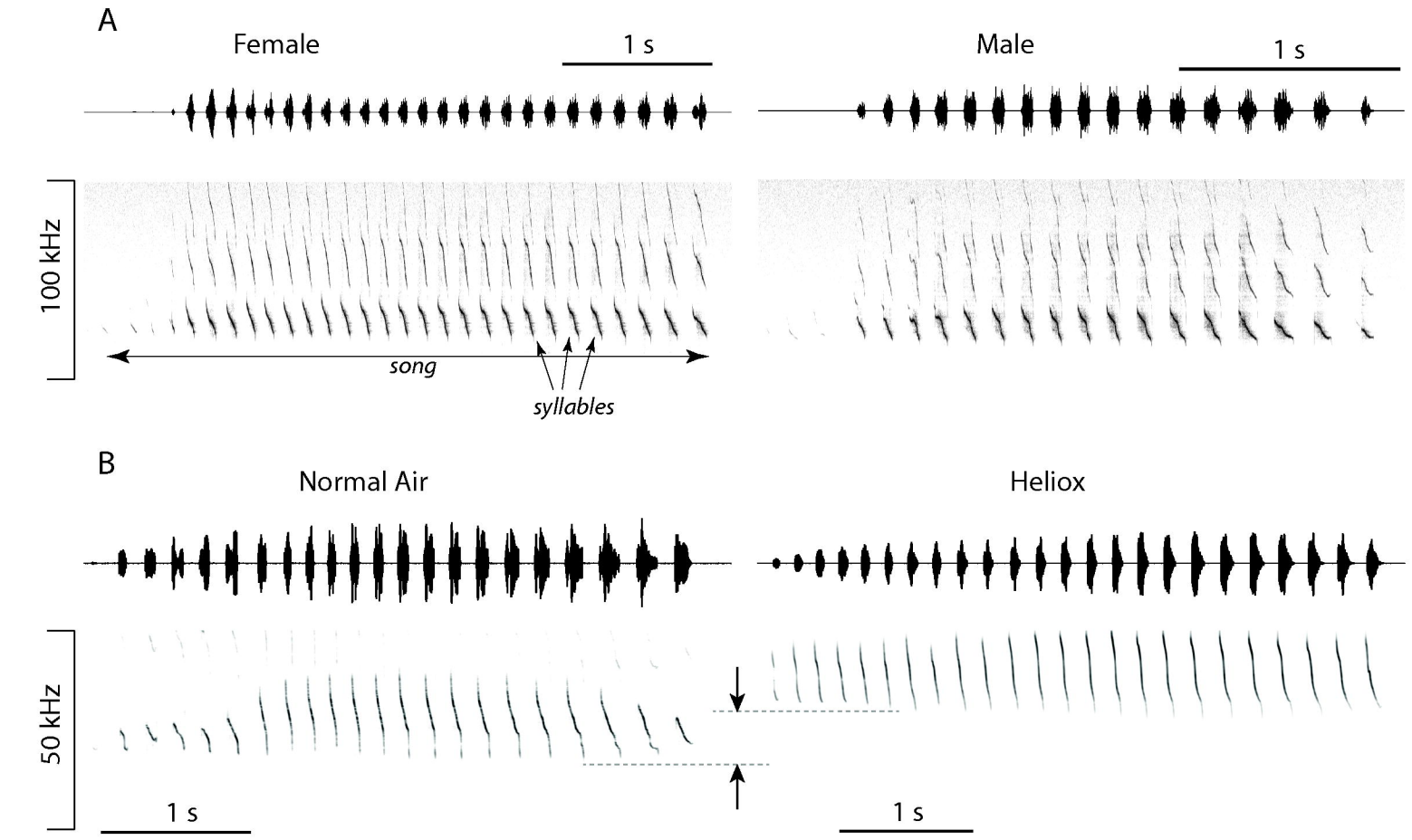
A
Female
1 s
Male
1 s
100 kHz
song
syllables
B
Normal Air
Heliox
50 kHz
1 s
1 s

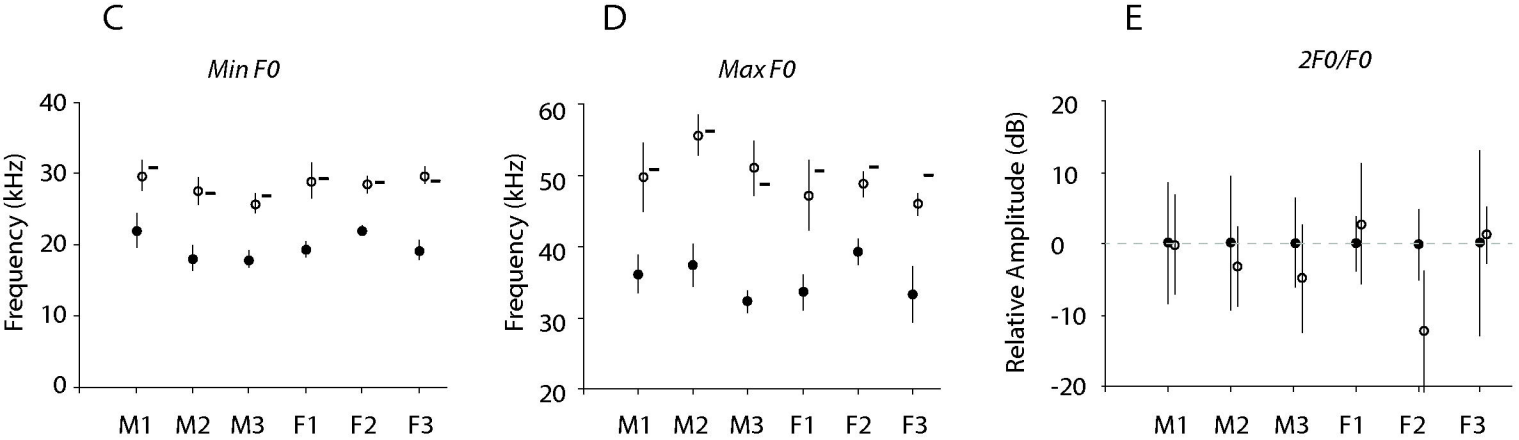
C
Min F0
Frequency (kHz)
40
30
20
10
0
M1 M2 M3 F1 F2 F3
D
Max F0
Frequency (kHz)
60
50
40
30
20
M1 M2 M3 F1 F2 F3
E
2F0/F0
Relative Amplitude (dB)
20
10
0
-10
-20
M1 M2 M3 F1 F2 F3

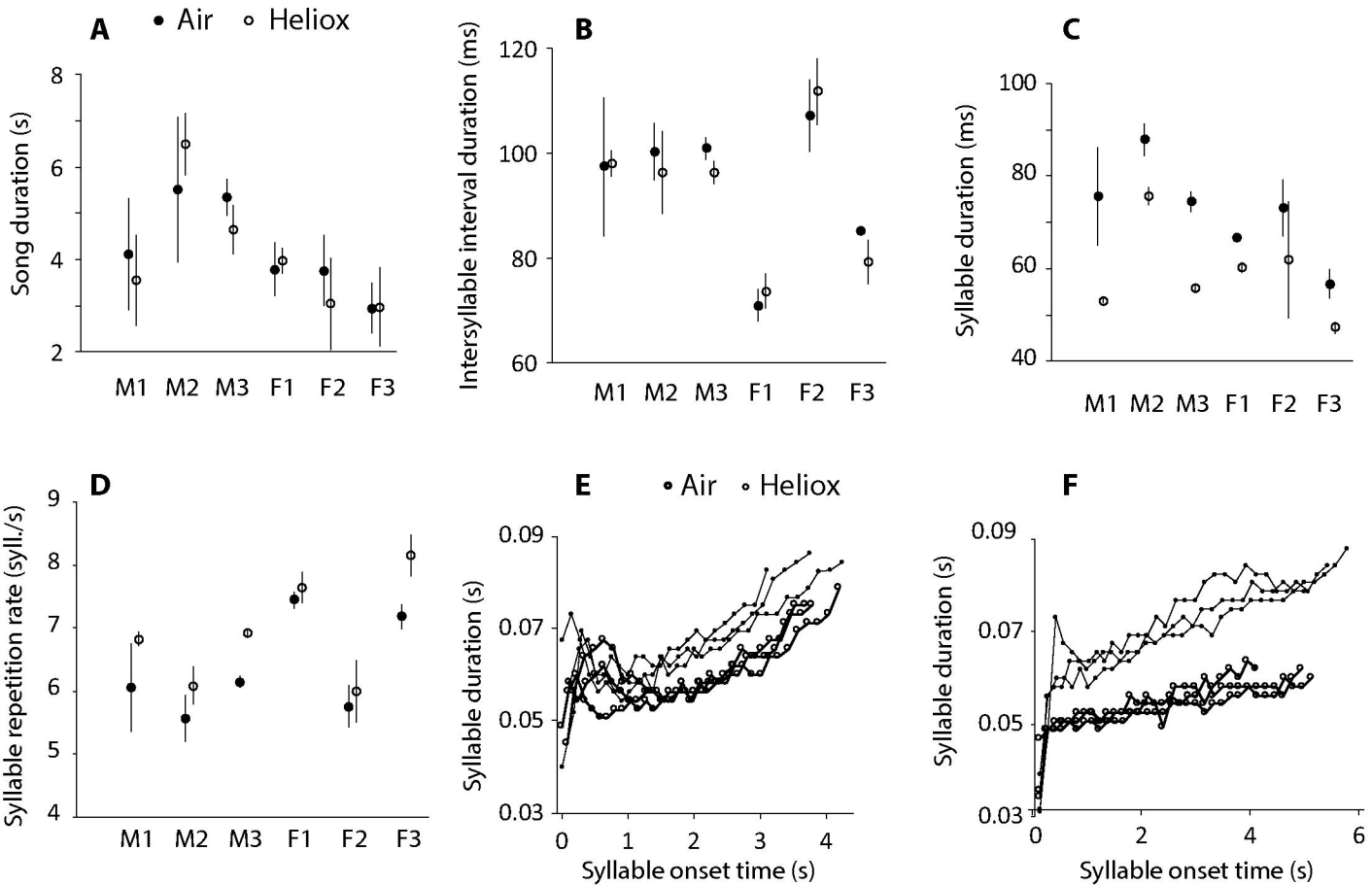
A
Air
Heliox
Song duration (s)
8
6
4
2
M1 M2 M3 F1 F2 F3
B
Intersyllable interval duration (ms)
120
100
80
60
M1 M2 M3 F1 F2 F3
C
Syllable duration (ms)
100
80
60
40
M1 M2 M3 F1 F2 F3
D
Syllable repetition rate (syll./s)
9
8
7
6
5
4
M1 M2 M3 F1 F2 F3
E
Air
Heliox
Syllable duration (s)
0.09
0.07
0.05
0.03
0 1 2 3 4
Syllable onset time (s)
F
Syllable duration (s)
0.09
0.07
0.05
0.03
0 2 4 6
Syllable onset time (s)

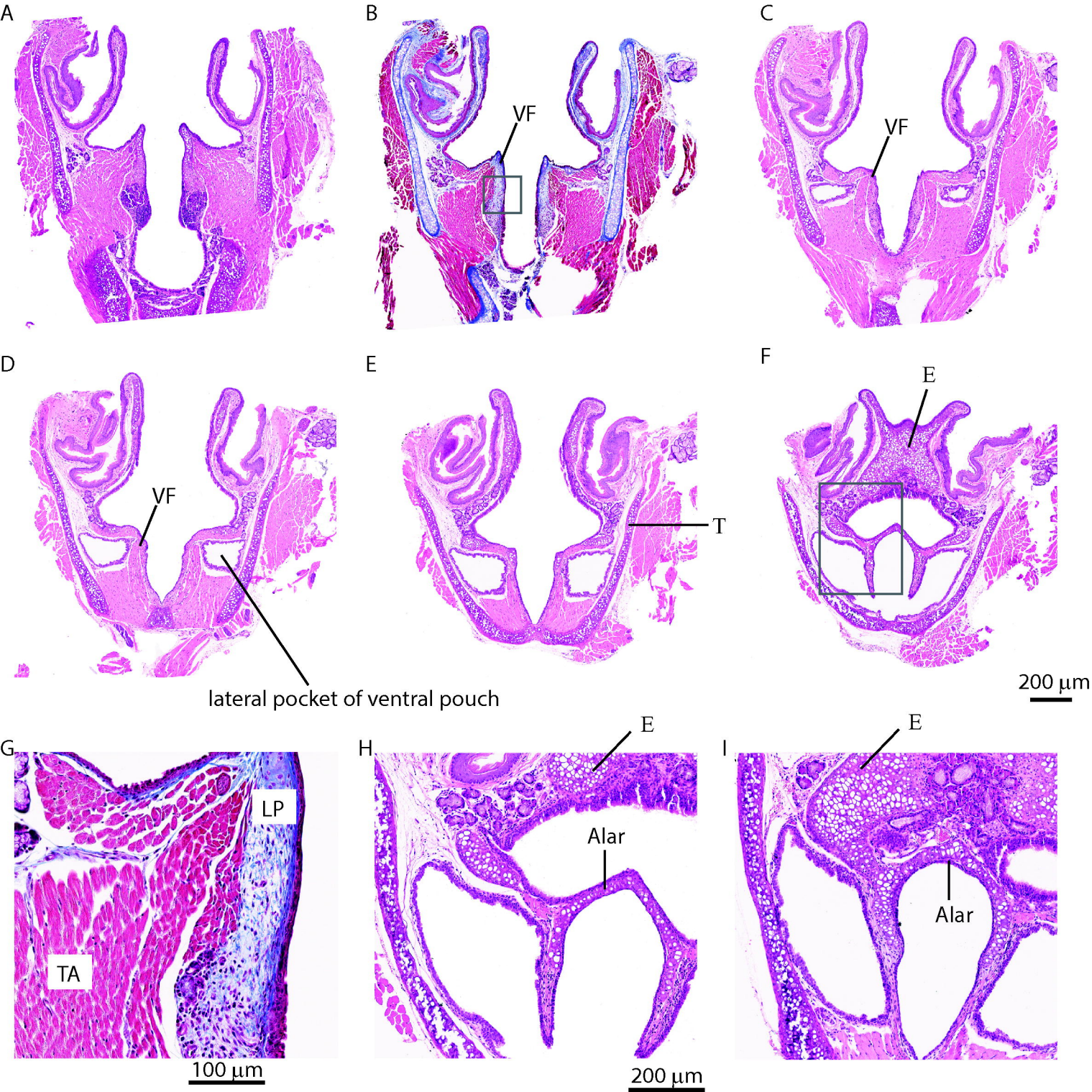
A
B
VF
C
VF
D
VF
lateral pocket of ventral pouch
E
T
F
E
200 µm
G
LP
TA
100 µm
H
E
Alar
200 µm
I
E
Alar

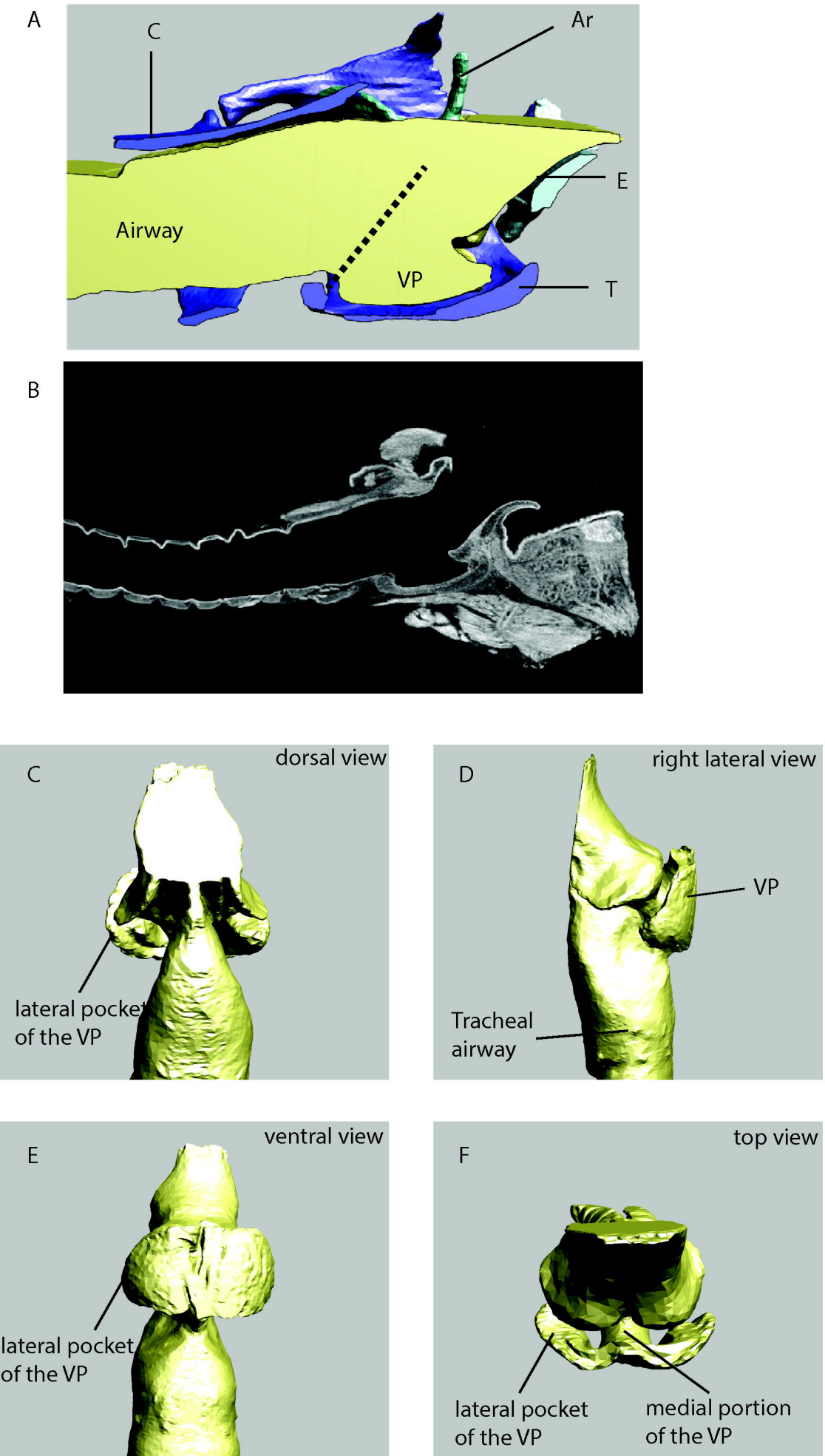
A
C
Ar
E
Airway
VP
T
B
C
dorsal view
lateral pocket
of the VP
D
right lateral view
VP
Tracheal
airway
E
ventral view
lateral pocket
of the VP
F
top view
lateral pocket
of the VP
medial portion
of the VP

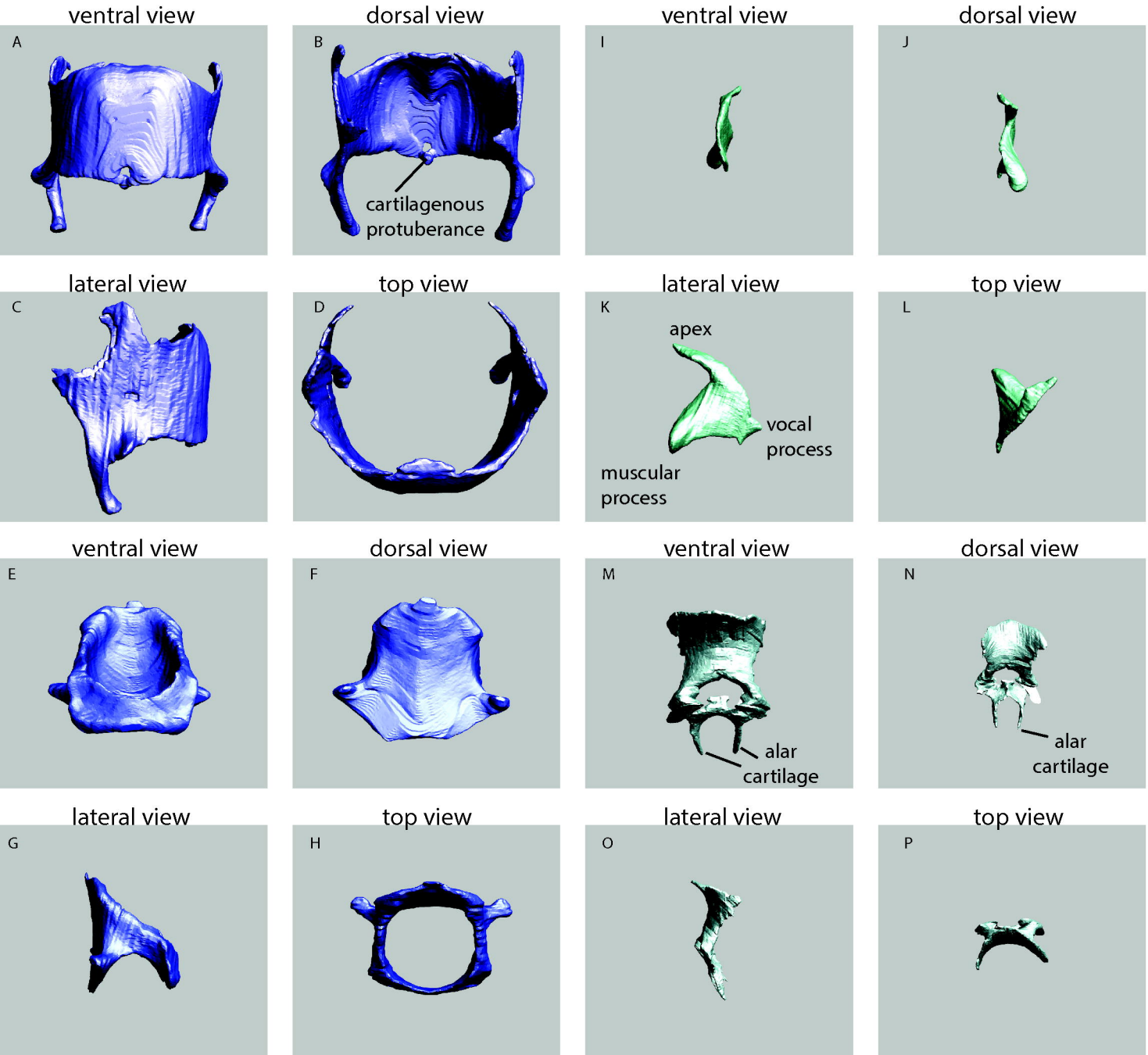
ventral view
dorsal view
ventral view
dorsal view
A
B
I
J
cartilagenous
protuberance
lateral view
top view
lateral view
top view
C
D
K
L
apex
vocal
process
muscular
process
ventral view
dorsal view
ventral view
dorsal view
E
F
M
N
alar
cartilage
alar
cartilage
lateral view
top view
lateral view
top view
G
H
O
P

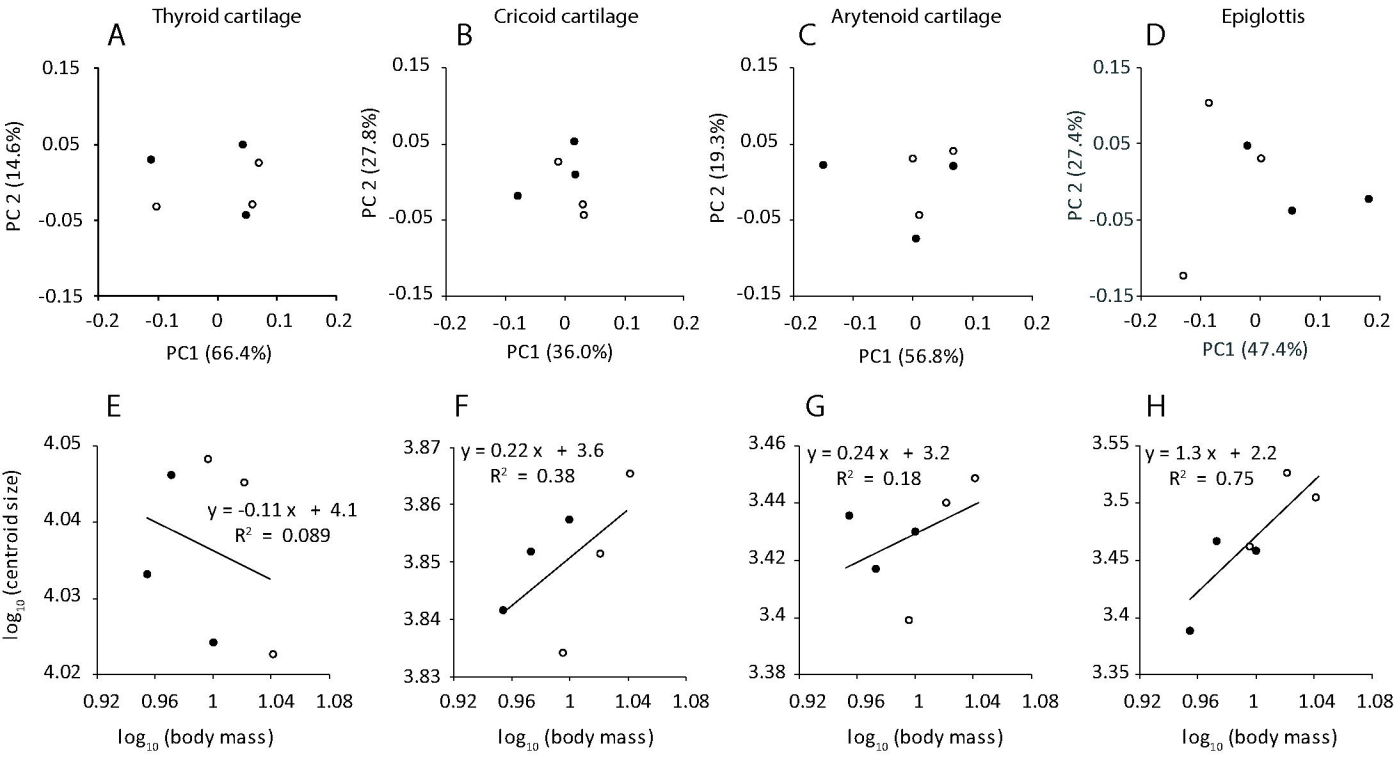
A
Thyroid cartilage
PC 2 (14.6%)
PC1 (66.4%)
B
Cricoid cartilage
PC 2 (27.8%)
PC1 (36.0%)
C
Arytenoid cartilage
PC 2 (19.3%)
PC1 (56.8%)
D
Epiglottis
PC 2 (27.4%)
PC1 (47.4%)
E
y = -0.11 x + 4.1
R² = 0.089
F
y = 0.22 x + 3.6
R² = 0.38
G
y = 0.24 x + 3.2
R² = 0.18
H
y = 1.3 x + 2.2
R² = 0.75
log10 (centroid size)
log10 (body mass)

Ventral pouch shape

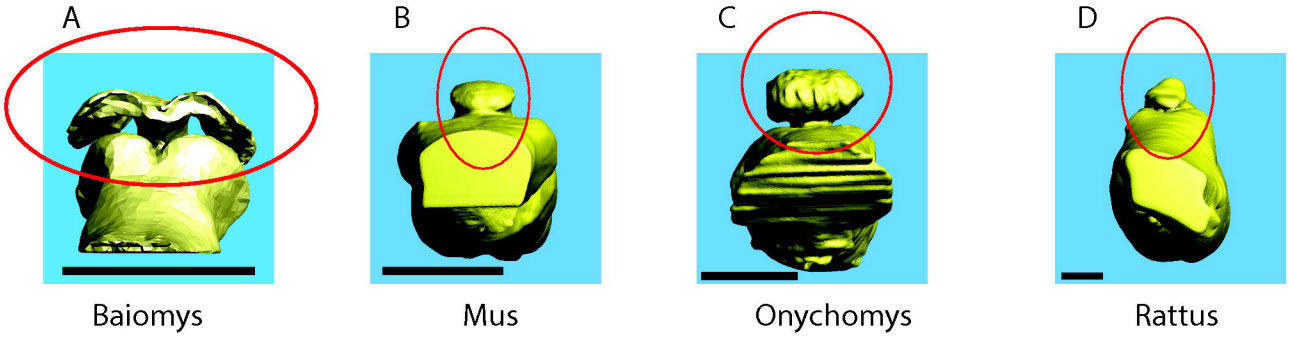

Larynx size

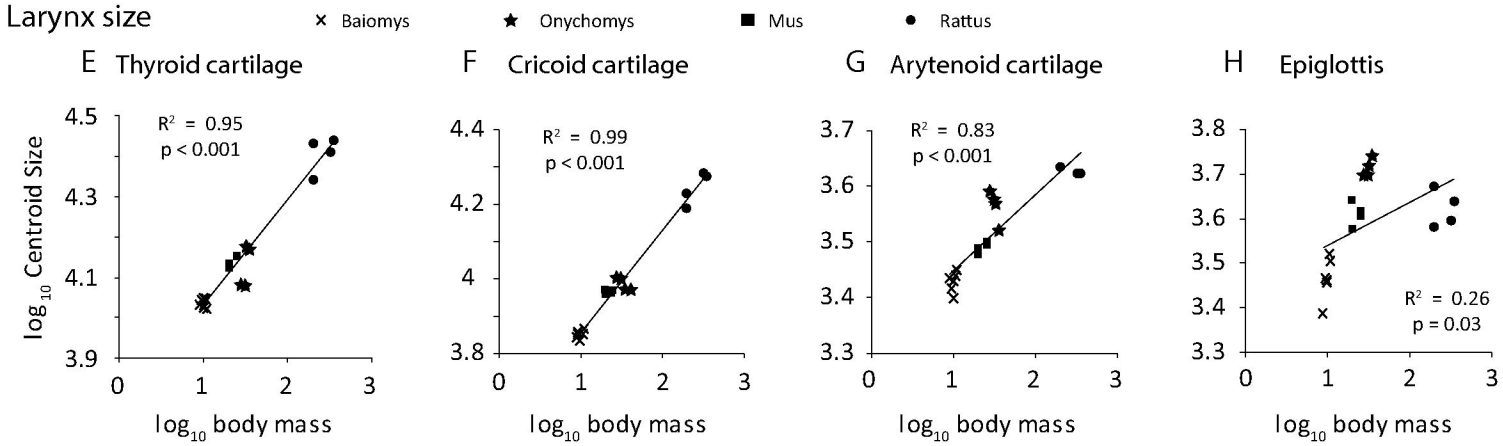

Ventral pouch size